ASEG-PESA 2013
'THE EUREKA MOMENT'
11-14 AUGUST 2013 • MELBOURNE, AUSTRALIA

Structure-coupled joint inversion for magnetotelluric, seismic refraction and reflection traveltime data

Xu Liu
University of Adelaide
North Terrace, Adelaide SA 5005
xu.liu@adelaide.edu.au

Graham Heinson
University of Adelaide
North Terrace, Adelaide SA 5005
graham.heinson@adelaide.edu.au

Bing Zhou
University of Adelaide
North Terrace, Adelaide SA 5005
bing.zhou@adelaide.edu.au

SUMMARY

A method of joint inversion of Magnetotelluric, seismic refraction and seismic reflection (JIMRR) is developed especially for typical hydrocarbon or hard-rock mineral exploration. JIMRR includes two parts: jointed seismic refraction and seismic reflection; and its combination with Magnetotelluric (MT) method. The objective of the research is to enhance spatial resolution of the three model parameters: electrical resistivity, seismic velocity and reflector depth. Since horizontal coordinates of reflector are not treated as model parameters in existing travel time inversion algorithm, seismic forward modelling may loss the true reflection point locations at the side edges of reflector with limited extension. We developed the technology of extensible reflector to overcome this problem. JIMRR is completed by employing the cross-gradient function as constraints which enforces the structural similarity between the resistivity and the seismic velocities, so as to reduce velocity-depth ambiguity. The cross-gradient constraints are incorporated into the solution through least squares and Lagrange multiplier method. This method results in integrated symmetric square linear matrix that is solved by bi-conjugate gradient method (BiCG). Two example synthetic models show that our joint inversion can significantly enhance the spatial resolution of inversion; and also the velocity-depth ambiguity caused by reflection travel time inversion can be notably reduced by constraints from shallow lithologies.

Key words: inversion, magnetotellurics, refraction and reflection seismology.

INTRODUCTION

Seismic and MT methods are important combination; seismic inversion reconstructs complex geologic structure and provide high-resolution of boundaries while MT methods provide the volumetric properties of electrical resistivity. To apply joint inversion of different physical data, certain relationships linking the different model parameters must be determined in advance. We call this type of relationships as cross-constraints so as to distinguish with the constraints used in the separate inversion. The current cross-constraints include direct relationships among physical parameters (e.g. Roecker et al. 2004), same structure border for those physical properties (e.g. Lines et al. 1988; Afnimar et al. 2002), and structure similarity (Gallardo and Meju, 2004, 2007). Gallardo and Meju (2007) presented the first joint 2-D inversion approach for imaging collocated MT and seismic refraction data with cross-gradient constraints and led to improve the structural conformity between the geophysical images. This method is extended to include seismic reflection data in JIMRR. A few of papers (Huang et al, 2012; Korenaga et al, 2000, Korenaga, 2011; Zhang et al, 1998) investigated the method of joint inversion of seismic refraction and reflection (JIRR). In terms of reflection tomography, a major concern is the existence of velocity-depth ambiguity and even in the JIRR (Sain and Kaila, 1996; Korenaga et al, 2000). In the JIRR method, the horizontal coordinates of reflector nodes are fixed so that each node has only one degree of freedom in the vertical direction. It is important to note that reflectors in their models cross the whole model and the end points are located at the side edges of the model.

To the best of our knowledge, no or very few papers integrated MT with seismic refraction and reflection. Therefore, our joint inversion equations are presented firstly. Then, the concepts of extensible reflector and shallow constrains are introduced. In the end, the effectiveness and resolution characteristics of this method are demonstrated with synthetic examples.

METHOD AND RESULTS

The joint inversion equations are

$$\begin{bmatrix} w^t \underline{\underline{\mathbf{G}}}^t & \mathbf{0} & \mathbf{0} & w^t \left(\mathbf{S}^t\right)^T \\ \mathbf{0} & \underline{\underline{\mathbf{G}}}^f + \left(\mathbf{G}^{rv}\right)^T \mathbf{G}^{rv} & w^d \left(\mathbf{G}^{rv}\right)^T \mathbf{G}^{rd} & \left(\mathbf{S}^v\right)^T \\ \mathbf{0} & \left(\mathbf{G}^{rd}\right)^T \mathbf{G}^{rv} & w^d \underline{\underline{\mathbf{G}}}^d & \mathbf{0} \\ w^t \mathbf{S}^t & \mathbf{S}^v & \mathbf{0} & \mathbf{0} \end{bmatrix} \begin{bmatrix} \frac{1}{w^t}\mathbf{m}^e \\ \mathbf{m}^v \\ \frac{1}{w^d}\mathbf{m}^d \\ \boldsymbol{\lambda} \end{bmatrix} = \begin{bmatrix} \left(\mathbf{G}^t\right)^T \hat{\mathbf{d}}^t + \mu^e \left(\mathbf{D}^e\right)^T \mathbf{D}^e \mathbf{m}_0^e \\ \left(\mathbf{G}^f\right)^T \hat{\mathbf{d}}^f + \left(\mathbf{G}^{rv}\right)^T \hat{\mathbf{d}}^r + \mu^v \left(\mathbf{D}^v\right)^T \mathbf{D}^v \mathbf{m}_0^v \\ \left(\mathbf{G}^{rd}\right)^T \hat{\mathbf{d}}^r + \mu^d \left(\mathbf{D}^d\right)^T \mathbf{D}^d \mathbf{m}_0^d \\ \hat{\mathbf{h}} \end{bmatrix}, \quad (1)$$

here

$$\underline{\underline{\mathbf{G}}}^t = \left(\mathbf{G}^t\right)^T \mathbf{G}^t + \alpha^e \left[\left(\mathbf{L}_h^e\right)^T \mathbf{L}_h^e + \left(\mathbf{L}_v^e\right)^T \mathbf{L}_v^e \right] + \mu^e \left(\mathbf{D}^e\right)^T \mathbf{D}^e, \quad (2)$$

$$\underline{\underline{\mathbf{G}}}^f = \left(\mathbf{G}^f\right)^T \mathbf{G}^f + \alpha^v \left[\left(\mathbf{L}_h^v\right)^T \mathbf{L}_h^v + \left(\mathbf{L}_v^v\right)^T \mathbf{L}_v^v \right] + \mu^v \left(\mathbf{D}^v\right)^T \mathbf{D}^v, \quad (3)$$

$$\underline{\underline{\mathbf{G}}}^d = \left(\mathbf{G}^{rd}\right)^T \mathbf{G}^{rd} + \alpha^d \left(\mathbf{L}^d\right)^T \mathbf{L}^d + \mu^d \left(\mathbf{D}^d\right)^T \mathbf{D}^d. \quad (4)$$

The superscripts t, f, r stand for MT, seismic refraction and seismic reflection methods; and e, v, d for electrical resistivity, seismic velocity and reflector depth respectively; $\mathbf{m}^{e,v,d}$, model parameter vectors; $\mathbf{L}_{h,v}^{e,v}$ are horizontal and vertical smoothing matrices; $\mathbf{L}^d$, smoothing matrices for

reflector depth; $\mathbf{D}^{e,v,d}$, damping matrixes; $\mathbf{m}_0^{e,v,d}$, the initial models (and thereafter to the previous iterate); $\mathbf{F}^t(\mathbf{m}_0^e)$ and $\mathbf{G}^t$,calculated MT data and MT Jacobian matrixes respectively; $\mathbf{F}^f(\mathbf{m}_0^v)$ and $\mathbf{F}^r(\mathbf{m}_0^v,\mathbf{m}_0^d)$, calculated refraction and reflection travel times respectively, and their Jacobian matrixes to velocity are $\mathbf{G}^f$, $\mathbf{G}^{rv}$; $\mathbf{G}^{rd}$,Jacobian matrix of seismic reflection to reflector depth and calculated by the formula of Zelt and Smith (1992); $\hat{\mathbf{d}}^{t,f,r}$, observed data $\mathbf{d}^{t,f,r}$ in jumping strategy form;

$$\left.\begin{aligned}\hat{\mathbf{d}}^t &= \mathbf{d}^t - \mathbf{F}^t(\mathbf{m}_0^e) + \mathbf{G}^t\mathbf{m}_0^e, \hat{\mathbf{d}}^f = \mathbf{d}^f - \mathbf{F}^f(\mathbf{m}_0^v) + \mathbf{G}^f\mathbf{m}_0^v \\ \hat{\mathbf{d}}^r &= \mathbf{d}^r - \mathbf{F}^r(\mathbf{m}_0^v,\mathbf{m}_0^d) + \mathbf{G}^{rv}\mathbf{m}_0^v + \mathbf{G}^{rd}\mathbf{m}_0^d\end{aligned}\right\}; \quad (5)$$

$\mathbf{S}^{e,v}$ and $\hat{\mathbf{h}}$ are vectors of cross-gradient constraints(Gallardo and Meju, 2004) in jumping strategy form

$$\hat{\mathbf{h}} = \mathbf{h} + \left[\mathbf{S}^e \quad \mathbf{S}^v\right]\left[\mathbf{m}_0^e \quad \mathbf{m}_0^v\right]^T; \quad (6)$$

w^t and w^d are the weighting factors; $\boldsymbol{\lambda}$ are Lagrange multiplier vector. The joint inversion equation (11) can be solved by bi-conjugate gradient method (BiCG).

Note that the horizontal coordinates of the reflector are not updated by the equation (1). However, for a typical survey profile in the hydrocarbon or hard-rock mineral exploration, the seismic source-receiver offset is between zero and 3 km, and the reflection data may come from anomalies with every size (causing scattering wave for low frequencies). This means that nodes at an end of a reflector may not be at a side edge of the model. Then, the true reflection points around the end node of the reflector are very possible outside the horizontal extension of the reflector. In this case, the forward modelling (ray-trace) codes have to choose the nodes inside the reflector (according to shortest ray path) or merge with other reflection points. This may cause inversion divergence. This problem is solved by our extensible reflector method. An extensible reflector is similar to the reflector defined by Korenaga et al. (2000). But the end nodes of extensible reflector are not necessarily at the side edges of the model. For every inversion iterate, ray-tracing identifies the reflection nodes for each seismic ray corresponding and connecting to each seismic detector. Those reflection nodes constitute an array of linear segments. Along this array, a short horizontal extension is made to the end reflection nodes (if not at the edge of the model). Then, interpolation is applied to make an updated reflector.

The reason of velocity-depth ambiguity in JIRR is that the lower rock velocity is mainly resolved only by reflection traveltimes (Korenaga et al. 2000). In other words, the first arrivals or refraction traveltimes do not contribute much to the nonuniqueness. However, the refraction can only resolve relatively shallow rocks. Therefore, we first determine the shallow velocity or shallow structure information through refraction inversion (or other additional methods: borehole logging, even wide angle reflection etc). The shallow velocity or shallow reflector structure are then fixed as the extra constraints in the procedures of joint inversion and is here called shallow constraints.

Two synthetic models, model 1 and model 2 (Fig. 1), are investigated. They have the same structure which is a rectangle anomaly block over an interface. But the seismic velocities (Vp) in the rectangle block are different (4.6 km/s for model 1 and 1.6 km/s for model 2). This model was viewed as an important illustration of velocity depth ambiguity by Bube et al (1995). Three reflectors (referred as: R1, R2 and R3) are applied to represent the top, the bottom of the anomaly block, and the low interface respectively. We presume that the seismic velocities within 100m deep and the depths of top reflector R1 are known as shallow constraints. The initial models of resistivity and velocity are homogenous (note the reflection traveltimes cannot resolve the velocity under the lowest reflector); the initial depths of reflectors R2 and R3 are both set at 100 m deeper than their true locations. The MT synthetic data are generated for 6 frequencies (3.2, 9.6, 28.8, 86.4, 259.2, 777.6 Hz) of 7 sounding sites. Seismic data are calculated for 33 seismic detectors of 4 seismic shot points. The seismic detectors are evenly spaced by 25m along the 800m profile as depicted in Fig. 1.

For model 1, the ray paths of seismic refraction are shown in Fig. 2. It is important to note that there is no ray coverage below reflector R1. Therefore, it is very hard to recover the velocities for the area below R1 by either seismic refraction or join MT and seismic refraction method. But, with the combination of seismic reflection waves, both the velocities and the interface are recovered by JIRR (Fig. 3(b)). However, our JIMRR gives even clearer results with higher resolution, see Fig. 3(d). Fig. 3(a) is the resistivity model inversed by single MT method. The shape of the rectangle block is also improved by the joint inversion; see Fig. 3(c). For model 2, the ray paths of seismic refraction are all along the surface. Therefore, it has to depend on the reflection waves to recover seismic structure. Even the shallow constraints need to be determined by the reflection waves from shallow reflectors (here R1, with the wide angle reflection). In this model, we also show the importance of the shallow constraints. Fig. 4(a) and Fig. 4(b) are the resistivity mode and seismic mode recovered by our JIMRR, but without shallow constraints. It is apparent that the inversion suffers from velocity-depth ambiguity and the rectangle block of velocity model is lower than its true position. However, they are much improved by the same joint inversion, but with the shallow constraints, see Fig. 4(c) and Fig. 4(d).

It is important to note that the interface (at 300m deep) is not recovered in the resistivity models by JIMRR in Fig. 3(c) and Fig. 4(c). The reason is that the interface corresponds to the lowest seismic reflector, below which there is no velocity information from traveltimes and cross-gradient constraints are still applied in this area. Therefore the lowest reflector determinates exploration depth of the joint inversion.

CONCLUSIONS

This study shows that JIMRR can significantly enhance the exploration depth; while it is very shallow if only seismic refraction is applies in the joint inversion for a typical seismic reflection profile. The method of extensible reflector is developed to allow JIMRR can be applied for multi-reflector with different extensions. The problem of velocity-depth ambiguity can be significantly reduced by applying shallow constraints. Two special synthetic models, although they are typically ambiguous, successfully demonstrate the advantages of JIMRR.

ACKNOWLEDGMENTS

We would like to appreciate the Deep Exploration Technologies Cooperative Research Centre (DET CRC) and ARC discovery project (DP1093110) for the sponsorship on this project.

REFERENCES

Afnimar, A., Koketsu, K. and Nakagawa, K., 2002, Joint inversion of refraction and gravity data for the three-dimensional topography of a sedimentbasement interface: Geophysical Journal Internationa., 151, 243–254.

Bube, K.P., Langan, R.T., and Resnick, J.R., 1995, Theoretical and numerical issues in the determination of reflector depths in seismic reflection tomography:: Journal of Geophysical Research, 100(B7), 12,449-12,458.

Constable, S., Key, K., and Myer, D., 2007, OCCAM 3.0 release notes: http://marineemlab.ucsd.edu/Projects/Occam/ (accessed on Feb. 2012)

Gallardo, L.A., and Meju, M.A., 2004, Joint two-dimensional DC resistivity and seismic travel time inversion with cross-gradients constraints: Journal of Geophysical Research: Solid Earth, 109, B03311, doi:10.1029/2003JB002716.

Gallardo, L.A. and Meju, M.A., 2007, Joint two-dimensional cross-gradient imaging of magnetotelluric and seismic traveltime data for structural and lithological classification: Geophysical Journal International, 169, 1261-1272.

Huang, G.J., Bai, C.Y., Zhu, D.L., and Greenhalgh, S., 2012, 2D/3D Seismic Simultaneous Inversion for the Velocity and Interface Geometry Using Multiple Classes of Arrivals: Bulletin of the Seismological Society of America, 102(2), 790-801.

Korenaga, J. 2011, Velocity–depth ambiguity and the seismic structure of large igneous provinces: a case study from the Ontong Java Platea: Geophysical Journal International, 185, 1022-1036.

Korenaga, J., Holbrook, W.S., Kent, G.M., Kelemen, P.B., Detrick, R.S., Larsens, H.C., Hoppesr, J.R. and Dahl-Jensse, T., 2000, Crustal structure of the southeast Greenland margin from joint refraction and reflection seismic tomography: Journal of Geophysical Research, 105(B9),21,591-21,614.

Lines, L. R., Schultz, A. K. and Treitel, S., 1988, Cooperative inversion of geophysical-data: Geophysics, 53, 8–20.

Roecker, S., Thurber, C. and McPhee, D., 2004, Joint inversion of gravity and arrival time data from Parkfield: New constraints on structure and hypocenter locations near the SAFOD drill site, Geophysical Research Letters, 31(12), L12S04, doi:10.1029/2003GL019396.

Said, K., and Kaila, K.L., 1996, Ambiguity in the solution to the velocity inversion problem and a solution by joint inversion of seismic refraction and wide-angle reflection times: Geophysical Journal International, 124, 125-227.

Zelt, C.A., and Smith, R.B., 1992, Seismic traveltime inversion for 2-D crustal velocity structure: Geophysical Journal International, 108, 16–34.

Zhang J., Brink, U.S.T., and Toksoz, M.N., 1998, Nonlinear refraction and reflection travel time tomography: Journal of Geophysical Research, 103(2), 29,743-29,757.

Zhou, B., and Greenhalgh, S.A., 2005, Shortest path ray tracing for the most general 2D/3D anisotropic media: Journal of Geophysical Engineering, 2, 54–63.

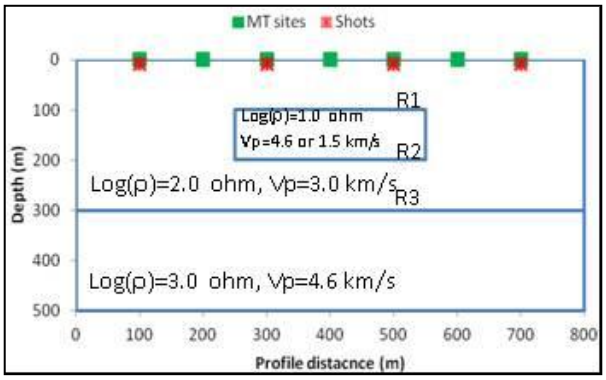

Figure 1. Synthetic test model 1 and model 2 have same structure and measure 500m by 800m with grad spacing 50m by 50m. The structure has a rectangle anomaly block over an interface. On the surface, the 7 green squares denote MT sounding sites and the 4 red crossed squares mark the seismic shots points. There are 33 seismic detectors located at the surface distances from 0 to 800m. The numbers in the model are the logarithm of resistivities and the seismic P-wave velocities. R1, R2 and R3 denote 3 reflectors corresponding to the top, the bottom of the anomaly and the interface respectively. The velocities (Vp) in the rectangle block are 4.6 km/s for model 1 and 1.5 km/s for model 2.

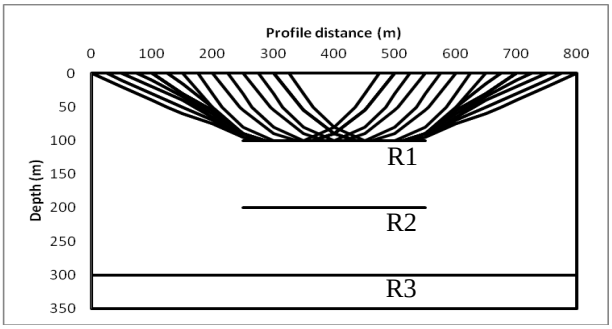

Figure 2. Ray path of seismic refraction of model 1. There is no ray coverage below R1 reflector. Therefore it is impossible to get information of velocity and structure below R1 reflector with joint MT and seismic refraction.

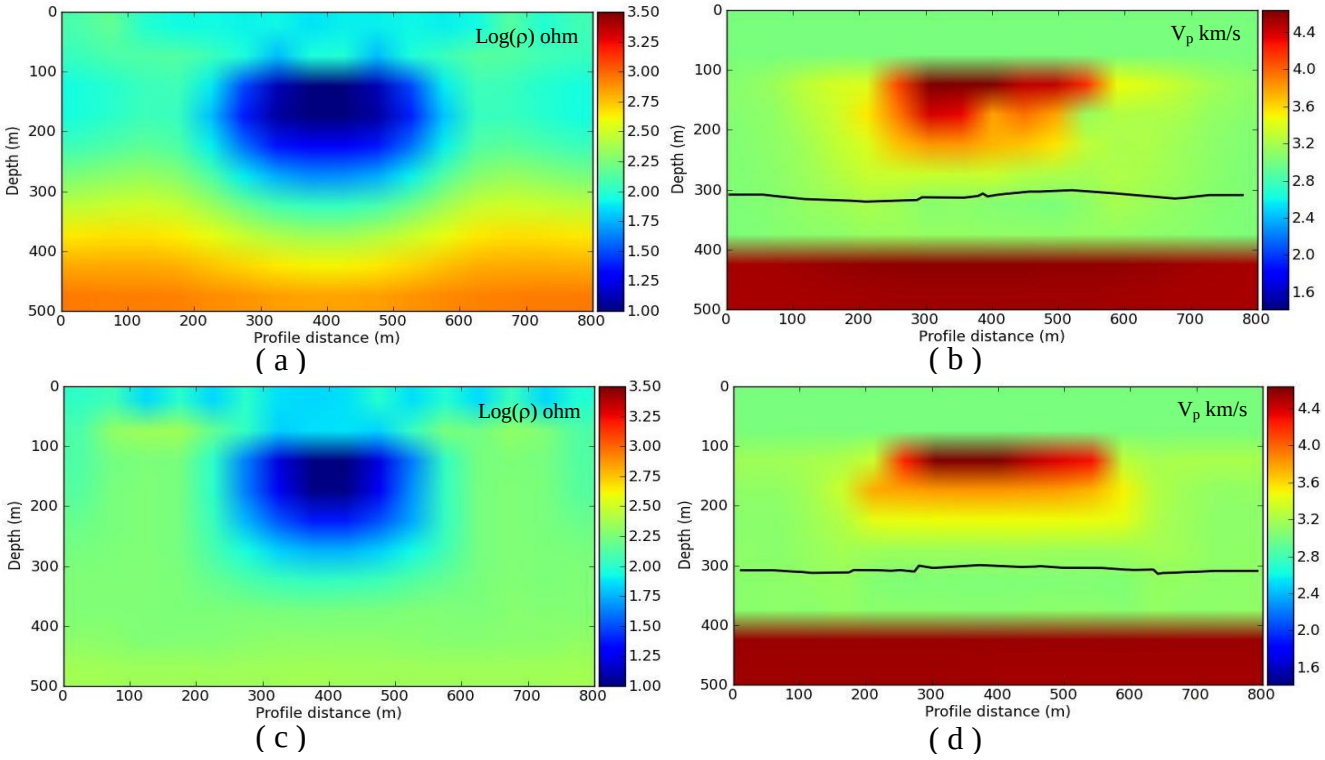

Figure 3. Model 1. (a) MT-resistivity model recovered by separate inversion using the source code of OCCAM3.0 (Constable et al. , 2007). (b) Seismic model obtained by separate seismic inversion of joint refraction and reflection with the source code based on Zhou and Greenhalgh (2005). (c) MT-resistivity and (d) seismic velocity models recovered by JIMRR. The black curves in (b) and (d) denote recovered interface

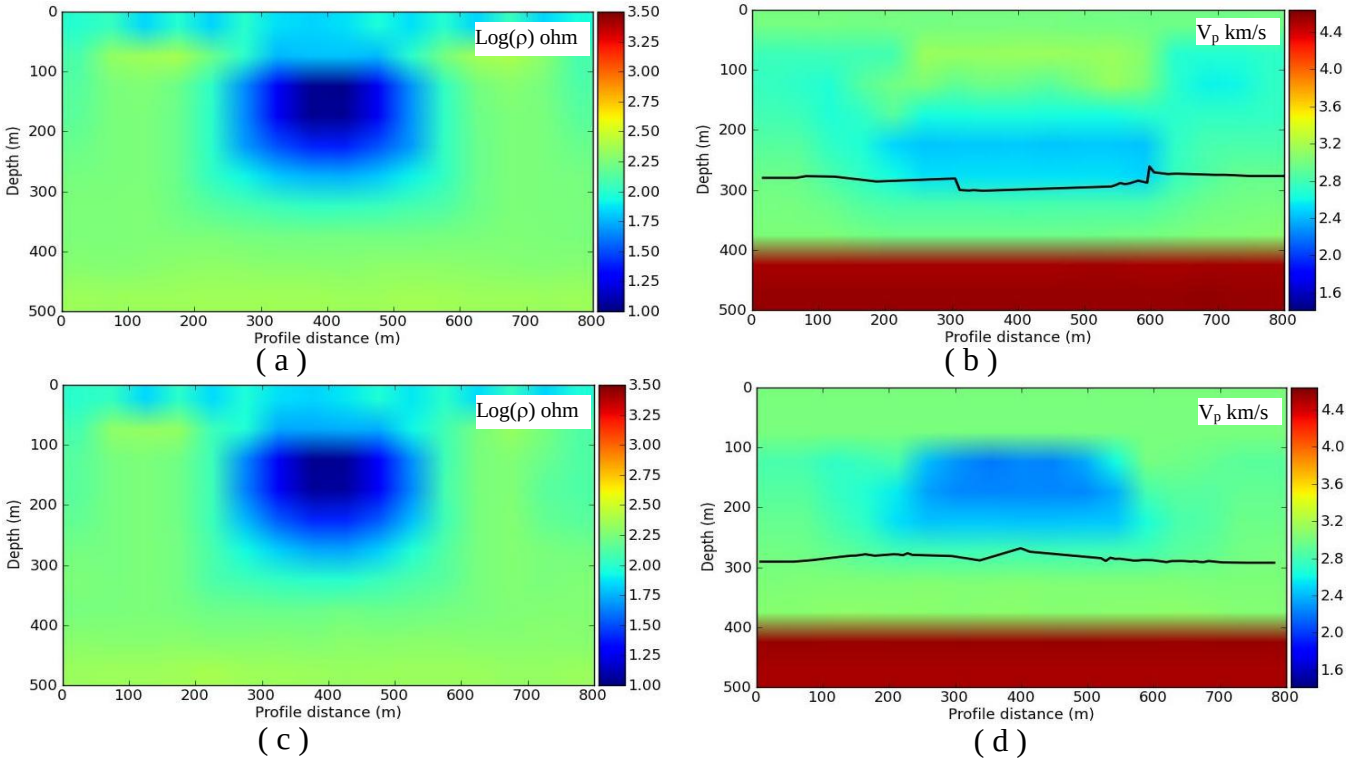

Figure 4. Model 2. (a) MT-resistivity and (b) seismic velocity models and interface recovered by JIMRR but without shallow constraints. (c) MT-resistivity and (d) seismic velocity model recovered by JIMRR. The black curves in (b) and (d) denote recovered interfaces.